

One-Dimensional Stochastic Lévy–Lorentz Gas.

E. Barkai^a, V. Fleurov^a and J. Klafter^b

^a School of Physics and Astronomy

^b School of Chemistry

Beverly and Raymond Sackler Faculty of Exact Sciences

Tel-Aviv University

Tel-Aviv 69978, Israel

(November 18, 2018)

We introduce a Lévy–Lorentz gas in which a light particle is scattered by static point scatterers arranged on a line. We investigate the case where the intervals between scatterers $\{\xi_i\}$ are independent random variables identically distributed according to the probability density function $\mu(\xi) \sim \xi^{-(1+\gamma)}$. We show that under certain conditions the mean square displacement of the particle obeys $\langle x^2(t) \rangle \geq Ct^{3-\gamma}$ for $1 < \gamma < 2$. This behavior is compatible with a renewal Lévy walk scheme. We discuss the importance of rare events in the proper characterization of the diffusion process.

PACS numbers: 02.50.-r, 05.40.+j, 05.60.+w

I. INTRODUCTION

In recent years there has been a growing interest in anomalous diffusion defined by

$$\langle x^2 \rangle = D_\delta t^\delta \quad (1)$$

and $\delta > 1$ [1–4]. Such a behavior was found in chaotic diffusion in low dimensional systems [5,6], tracer diffusion in a rotating flow [7], N body Hamiltonian dynamics [8], Lorentz gas with infinite horizon [1,9] and diffusion in egg crate potentials [10]. In all these examples one observes long ballistic flights in which the diffusing particle moves at a constant velocity. The transport is characterized by a distribution of free flight times which follows a power law decay. These processes have been usually analyzed using the Lévy walk framework (see more details below) [2–4,6].

It has been recently suggested by Levitz [11] that three-dimensional molecular Knudsen diffusion, at very low pressures, inside porous media can be described by Lévy walks. It has been also shown [12] that pore chord distributions, in certain three-dimensional porous media decay as a power law, at least for several length scales. Hence one can anticipate that a light test particle injected into such a medium may exhibit a Lévy walk. This has motivated the investigation of a fractal Lorentz gas. Levitz [11] has simulated trajectories of a light particle

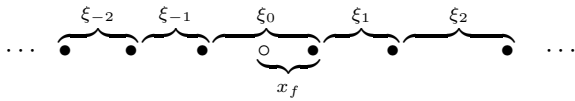
reflected from a three-dimensional intersection of a four-dimensional Weierstrass–Mandelbrot hyper surface, and found an enhanced Lévy type diffusion.

Here we investigate a one dimensional stochastic Lorentz gas which we call Lévy–Lorentz gas. In this model a light particle is scattered by a fixed array of identical scatterers arranged randomly on a line. Upon each collision event the light particle can be transmitted (or reflected) with probability T (or $R = 1 - T$). We investigate the case when the intervals between the scatterers are independent identically distributed random variables with a diverging variance.

We find: **(a)** a lower bound for the mean square displacement which is compatible with the Lévy walk model, and **(b)** that the generalized diffusion coefficient D_δ is very sensitive to the way the system has been prepared at time $t = 0$. As expected, we show that the transport is not Gaussian. In systems that exhibit normal diffusion, the contribution from ballistic motion, $x^2 = v^2 t^2$, is important only for short times; here we show that the ballistic motion cannot be neglected even at $t \rightarrow \infty$. The ballistic paths contribute to the generalized diffusion coefficient D_δ exhibiting a behavior different than normal.

II. MODEL AND NUMERICAL PROCEDURE

Assume a light particle which moves with a constant speed ($v = \pm 1$) among identical point scatterers arranged randomly on a line. Upon each collision, the probability that the light particle is transmitted (reflected) is T ($R = 1 - T$). The intervals between scattering points, $\xi_i > 0$ with $(i = \dots, -n, \dots, -1, 0, 1, \dots)$, are independent identically distributed random variables described by a probability density function $\mu(\xi)$. An important random variable is x_f defined to be the distance between the initial location of the light particle ($x = 0$) and the first scatterer in the sequence located at $x > 0$. The random variable x_f is described by the probability density function $h(x_f)$. A set of scatterers (black dots) is given schematically by:



$$\langle x^2 \rangle \sim \begin{cases} t^{3-\gamma}, & 1 < \gamma < 2 \\ t^2, & 0 < \gamma < 1. \end{cases} \quad (2)$$

where the open circle represents the light test particle at time $t = 0$. We consider the case when for large ξ , $\mu(\xi) \sim \xi^{-(1+\gamma)}$, with $0 < \gamma < 2$. Thus the variance of the length intervals $\{\xi_i\}$ diverges. A realization of the scatterers is shown in Fig. 1, for the case $\gamma = 3/2$. We observe large gaps which are of the order of the length of the system.

The case for which the variance converges has been investigated thoroughly in [13–17], resulting in: (i) a normal Gaussian diffusion as expected from the central limit theorem, and (ii) a $3/2$ power law decay in t of the velocity autocorrelation function.

Along this work we present numerical results for the case $\gamma = 3/2$ and $T = 1/2$. We use the following numerical procedure. First we generate a set of scatterers on a one dimensional lattice with a lattice spacing equal unity. Using a discrete time and space iteration scheme we find an exact expression for the probability of finding the particle on x at time t , $p(x, t|x = 0, t = 0)$, given that at $t = 0$ the particle is on $x = 0$. The initial location of the particle is determined using equilibrium initial conditions (see details below). The initial velocity is $v = 1$ or $v = -1$ with equal probabilities. $p(x, t|x = 0, t = 0)$ depends on the realization of disorder we have generated in the first step. This procedure is repeated many times.

In appendix A we explain how we generated the random intervals $\{\xi_i\}$. When $\gamma = 3/2$ the mean $\langle \xi \rangle \equiv \int_0^\infty \mu(\xi) d\xi$ is finite while the second moment $\langle \xi^2 \rangle = \infty$. Since $|v| = 1$ the characteristic microscopic time scale is $\langle \xi \rangle$ which is referred to as the mean collision time, and our simulations are for times $t \sim 1000 \langle \xi \rangle$. For our choice of parameters $\langle \xi \rangle \sim 4$ (see more details in Appendix A).

III. RESULTS

Let us analyze our one-dimensional Lévy–Lorentz model using the Lévy walk approach [2–4,6,18]. Lévy walks describe random walks which exhibit enhanced diffusion and are based on the generalized central limit theorem and Lévy stable distributions [19]. Briefly, a particle moves with a constant velocity $v = +1$ or $v = -1$ and then at a random time τ_1 its velocity is changed. Then the process is renewed. Each collision is independent of the previous collisions. The times between collision events $\{\tau_i\}$ are assumed to be independent identically distributed random variables, given in terms of a probability density function $q(\tau)$. One might expect that the dynamics of Lévy–Lorentz gas can be analyzed using the Lévy walk renewal approach with $q(\tau) \sim \tau^{-(1+\gamma)}$, for large τ and $0 < \gamma < 2$, which leads to

For $\gamma > 2$ one finds normal diffusion. It is clear that the renewal Lévy walk approach and the Lévy–Lorentz gas are very different. Within the Lévy–Lorentz gas collisions are not independent and correlations are important. Hence it is interesting to check whether the renewal Lévy walk model is suitable for the description of the Lévy–Lorentz gas. In this context it is interesting to recall that Sokolov et al [20] have shown that correlations between jumps in a Lévy flight in a chemical space destroy the Lévy statistics of the walk.

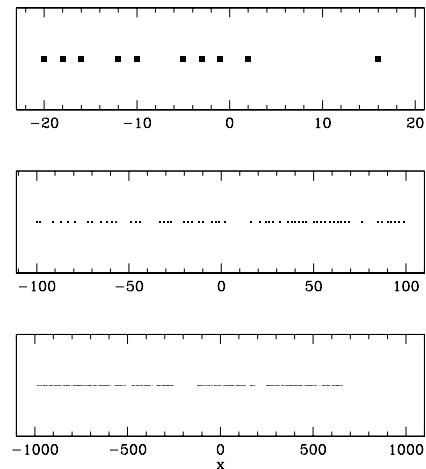


FIG. 1. A realization of a set of scatterers with $\gamma = 3/2$ exhibiting gaps on many scales. The horizontal axis is the x coordinate. All along this work we consider dimensionless units.

We consider a continuum model to derive our analytical results; the generalization to the lattice case is straightforward. Let $\langle p(x, t|x = 0, t = 0) \rangle dx$ be the probability, averaged over disorder, of finding the test particle at time t , in the interval $(x, x + dx)$. Initially, at time $t = 0$, the particle is at $x = 0$, and there is an equal probability of the particle having a velocity $v = +1$ or $v = -1$. Figs. 2 and 3 present numerical simulations which show $\langle p(x, t|x = 0, t = 0) \rangle$. One can see that in addition to the central peak on $x = 0$, two other peaks appear at locations $x = \pm t$. These peaks, known as ballistic peaks, were observed in a similar context in other systems exhibiting enhanced diffusion [6,11,21]. The peaks are stable on the time scale of the numerical simulation. The height of these peaks decays with time, and according to our finite time numerics the central peak and the ballistic peaks

decay according to the same power law when $\gamma = 3/2$.

Let us analyze analytically the time dependence of the ballistic peaks and calculate their contribution to the mean square displacement. Since in our model $|v| = 1$ it is clear that

$$\langle p(x, t | x = 0, t = 0) \rangle = 0, \quad \text{for } |x| > t. \quad (3)$$

We decompose the ensemble averaged probability density into two terms

$$\begin{aligned} \langle p(x, t | x = 0, t = 0) \rangle = \\ \langle \tilde{p}(x, t | x = 0, t = 0) \rangle + \frac{1}{2} Q_b(t) [\delta(x + t) + \delta(x - t)]. \end{aligned} \quad (4)$$

The first term on the RHS, $\langle \tilde{p}(x, t | x = 0, t = 0) \rangle$, is the probability density of finding the light particle at $|x| < t$. $Q_b(t)$ is the probability of finding the light particle at $x = t$ ($x = -t$) if initially at $x = 0$ and its velocity is $+1$ (-1). The left-right symmetry in Eq. (4) means that we have used the symmetric initial condition (i.e., $v = +1$ or $v = -1$ with equal probabilities) and the assumption that the system of scatterers is isotropic in an averaged sense. Using a similar notation we write

$$\langle x^2 \rangle = \langle \tilde{x}^2 \rangle + \langle x^2 \rangle_b, \quad (5)$$

where $\langle x^2 \rangle_b$ is the ballistic contribution to the mean square displacement. From Eq. (4) we have

$$Q_b(t) t^2 \leq \langle x^2(t) \rangle \leq t^2. \quad (6)$$

The upper bound is an obvious consequence of the fact that $|v| = 1$. The lower bound, found using $\langle x^2(t) \rangle_b \leq \langle x^2(t) \rangle$, is of no use when all moments of $\mu(\xi)$ converge, since then $Q_b(t)$ usually decays exponentially for long times. Eq. (6) is useful when the moments of $\mu(\xi)$ diverge, a case we consider here.

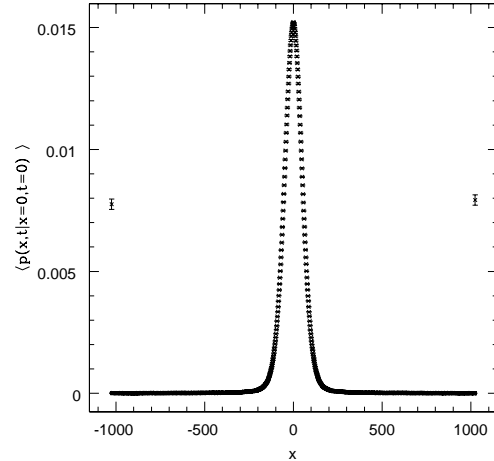


FIG. 2. A histogram presenting the $\langle p(x, t | x = 0, t = 0) \rangle$ versus x for time $t = 1024$, $\gamma = 3/2$ and $T = 1/2$. Notice the ballistic peaks of the propagator at $x = \pm t$. The average is over 1.8×10^5 realizations of disorder. The bin length is unity.

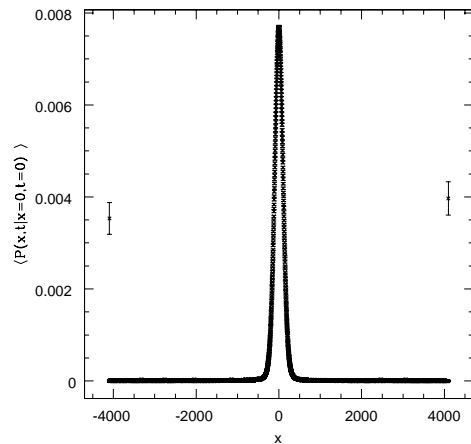


FIG. 3. The same as Fig. 2 for time $t = 4096$. The probability of finding a ballistic path, $\langle p(x = \pm t, t | x = 0, t = 0) \rangle \simeq 0.004$, is small but yet of statistical significance when $\langle x^2(t) \rangle$ is calculated.

To find $Q_b(t)$ consider a test particle which is initially of velocity $+1$ and located at $x = 0$. The probability it reaches $x = t$, at time t , is T^r where r is the number of scatterers in the interval of length $(0, t)$. Hence,

$$Q_b(t) = \sum_{r=0}^{\infty} T^r G_r(t), \quad (7)$$

and $G_r(t)$ is the probability of finding r scatterers in $(0, t)$. $G_r(t)$ can be calculated in terms of $\mu(\xi)$ and of $h(x_f)$. In appendix B we use renewal theory to calculate the Laplace $t \rightarrow u$ transform of $Q_b(t)$

$$\hat{Q}_b(u) = \frac{1}{u} + \frac{(T-1)\hat{h}(u)}{[1-T\hat{\mu}(u)]u}. \quad (8)$$

When $T = 1$, $\hat{Q}_b(u) = 1/u$, as expected from a transmitting set of scatterers. In deriving Eq. (8) we have used the model assumptions that the intervals $\{\xi_i\}$ are statistically independent and identically distributed.

The function $h(x_f)$ depends on the way the system of scatterers and light particle are initially prepared. Consider the following preparation process. A scatterer is assigned at the location $x = -L$ (eventually $L \rightarrow \infty$), then random independent length intervals are generated using the probability density $\mu(\xi)$. These length intervals determine the location of scatterers on the line. When the sum of the length intervals exceeds $2L$ the process is stopped. As mentioned, at time $t = 0$ the light particle is assigned to the point $x = 0$. When the mean distance between scatterers $\langle \xi \rangle = \int_0^\infty \xi \mu(\xi) d\xi$ converges (i.e., $1 < \gamma$), and $L \rightarrow \infty$ then according to [19,22]

$$h(x_f) = \frac{1 - \int_0^{x_f} \mu(\xi) d\xi}{\langle \xi \rangle}, \quad (9)$$

which is standard in the context of the Lorentz gas when the moments of $\mu(\xi)$ converge [13,15]. This type of initial condition is called equilibrium initial condition. When $1 < \gamma < 2$, Eq. (9) implies that $h(x_f) \sim (x_f)^{-\gamma}$ and hence $\langle x_f \rangle = \int_0^\infty x_f h(x_f) dx_f \rightarrow \infty$. At first sight this divergence might seem to be paradoxical, since the mean distance between scatterers, $\langle \xi \rangle$, converges. We notice however that the point $x = 0$ has a higher probability to be situated in a large gap. Hence, statistically the interval ξ_0 is much larger than the others and in our case $\langle x_f \rangle = \infty$. Eq. (9) implies that on average one has to wait an infinite time for the first collision event.

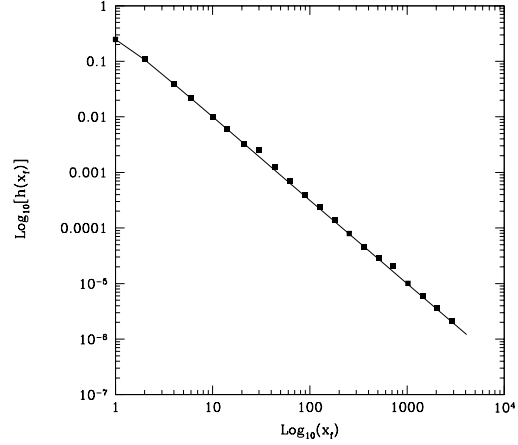


FIG. 4. The probability to find the first scatterer at a distance x_f from the origin. Here the average is over $3 * 10^5$ realizations, and half the length of the system is $L = 10^5$. We use a bin of length 32 (dimensionless units). The solid curve is the theoretical prediction, Eq. (9), with no fitting parameters. For large x_f , $h(x_f) \sim x_f^{-\gamma}$ and $\gamma = 3/2$, which implies that $\langle x_f \rangle$ diverges.

In numerical simulations the system's length L is finite, so that Eq. (9) is only an approximation which we expect to be valid for $x_f \ll L$. However, if we observe a system for time $t \ll L$ the boundary condition is not expected to influence the anomalous dynamics. We have generated numerically many random systems, using $\mu(\xi) \sim \xi^{-(1+\gamma)}$ and $\gamma = 3/2$. As shown in Fig. 4, $h(x_f) \sim (x_f)^{-\gamma}$ as predicted in Eq. (9).

We consider the small u expansion, of the Laplace transform of $\mu(\xi)$,

$$\hat{\mu}(u) = 1 - \langle \xi \rangle u + a (\langle \xi \rangle u)^\gamma \dots, \quad (10)$$

where $1 < \gamma < 2$ and a is a constant. Using a Tauberian theorem and Eqs. (8), (9) it can be shown that for long times t

$$Q_b(t) = \frac{a}{\Gamma(2-\gamma)} \left(\frac{t}{\langle \xi \rangle} \right)^{1-\gamma} + \frac{2a(\gamma-1)}{\Gamma(2-\gamma)} \frac{T}{1-T} \left(\frac{t}{\langle \xi \rangle} \right)^{-\gamma} + \dots \quad (11)$$

Inserting Eq. (11) in Eq. (6) we find

$$\frac{a \langle \xi \rangle^2}{\Gamma(2-\gamma)} \left(\frac{t}{\langle \xi \rangle} \right)^{3-\gamma} \leq \langle x^2(t) \rangle \leq t^2 \quad (12)$$

This bound demonstrates that the diffusion is enhanced, namely the mean square displacement increases faster than linearly with time.

In Fig. 5, we present the mean square displacement of the light particle obtained by numerical simulations for the case $\gamma = 3/2$. We see that for the chosen values of parameters the asymptotic $t^{3-\gamma}$ behavior can be observed for times which are accessible on our computer. Fig. 5 clearly shows that the ballistic contribution $\langle x^2 \rangle_b$ to the mean square displacement $\langle x^2 \rangle$ is significant. Notice that our numerical results are presented for times which are much larger than the mean collision time $\langle \xi \rangle \sim 4$.

In Fig. 6 we show the probability of finding a ballistic path, namely, the probability of finding the light particle at time t at $x = +t$, or at $x = -t$. By definition these probabilities are equal to $Q_b(t)/2$. We observe the $t^{1-\gamma}$ behavior of $Q_b(t)$, Eq. (11), with which our lower bound was found. The fact that the probability of finding the particle at $x = t$ is equal to the probability of finding the particle at $x = -t$ means that our system is isotropic in an averaged sense. This is achieved by choosing large values of L .

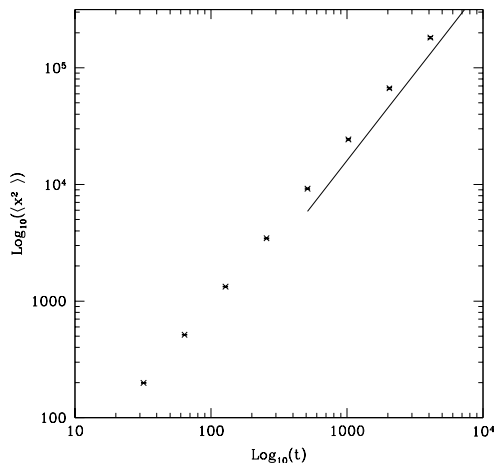


FIG. 5. $\log_{10} [\langle x^2 \rangle]$ versus $\log_{10}(t)$. The points are numerical results. The straight curve is the asymptotic behavior of the lower bound, Eq. (12) (i.e., $\langle x^2 \rangle_b$). We use $\gamma = 3/2$ and so $\langle x^2 \rangle \geq Ct^{3/2}$.

The lower bound in Eq. (12) does not depend on the transmission coefficient T . Thus, even when all the scatterers are perfect reflectors, with $R = 1$, the diffusion is enhanced. Large gaps which are of the order of the length t are responsible for this behavior. The transmission coefficient has an important role in determining what is the asymptotic time of the problem. The condition that the first term in Eq. (11) dominates over the second reads:

$$\frac{t}{\langle \xi \rangle} \gg 2(\gamma - 1) \frac{T}{1 - T}. \quad (13)$$

Only under this condition the behavior in Eq. (12) is expected to be valid.

The lower bound in Eq. (12) is compatible with the renewal Lévy walk approach Eq. (2). Other stochastic models [1,23] for enhanced diffusion based on Lévy scaling arguments predict

$$\langle x^2 \rangle \sim t^{2/\gamma} \quad \text{for } 1 < \gamma < 2 \quad (14)$$

which is different from Eq. (2). This approach is based upon a fractional Fokker-Planck equation (FFPE)

$$\frac{\partial p(x, t)}{\partial t} = D_\gamma \nabla^\gamma p(x, t) \quad (15)$$

used in [23] to predict an enhanced diffusion. The non-local fractional operator in Eq. (15) is defined in Fourier k space according to the transformation $\nabla^\gamma \rightarrow -|k|^\gamma$. Our findings here show that Eq. (14) does not describe the dynamics of the Lévy-Lorentz gas, since $3 - \gamma \geq 2/\gamma$ for $1 \leq \gamma \leq 2$.

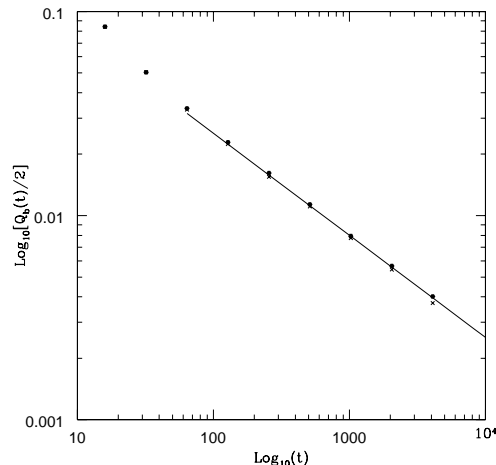


FIG. 6. The probability to find the light particle at time t at $x = +t$ (stars) and at $x = -t$ (dots) versus time. The solid curve is the theoretical prediction, Eq. (11) (no fitting parameters) which gives $Q_b(t)/2 \sim t^{1-\gamma}$, with $\gamma = 3/2$.

Consider now the case when the light particle is initially located at a scattering point. Such an initial condition is called non equilibrium initial condition. Under this condition $h(x_f) = \mu(x_f)$ instead of Eq. (9). This means that the particle has to wait an average time $\langle \xi \rangle$ before the first collision event instead of the infinite time when the equilibrium initial conditions were used. Using Eqs. (5), (8) and (10), and $\hat{\mu}(u) = 1 - (Au)^\gamma + \dots$ for $0 < \gamma < 1$ and small u , we find

$$\langle x^2 \rangle \geq \begin{cases} \frac{1}{1-T} a \frac{(\gamma-1)}{\Gamma(2-\gamma)} \langle \xi \rangle^2 \left(\frac{t}{\langle \xi \rangle} \right)^{2-\gamma}, & 1 < \gamma < 2 \\ \frac{1}{1-T} \frac{(1-\gamma)}{\Gamma(2-\gamma)} A^2 \left(\frac{t}{A} \right)^{2-\gamma}, & 0 < \gamma < 1. \end{cases} \quad (16)$$

For $1 < \gamma < 2$ the bound differs from the $t^{3-\gamma}$ found in Eq. (12), where we chose $h(x_f)$ according to Eq. (9). Thus the ballistic contribution $\langle x^2 \rangle_b$, defined in Eq. (5), behaves differently for the two ensembles even when $t \rightarrow \infty$. This is very different from regular Lorentz gases, which in the limit $t \rightarrow \infty$ are not sensitive to the choice of $h(x_f)$.

Finally, Fig. 7 shows the behavior of the correlation function $\langle p(x=0, t|x=0, t=0) \rangle$ obtained from the numerical simulation with equilibrium initial conditions. We observe a $t^{-1/2}$ decay of the correlation function. This behavior is compatible with standard Gaussian diffusion which gives the well known $t^{-d/2}$ result in d dimensions. We find this behavior for time scales which are much larger than the mean collision time $\langle \xi \rangle$, however we have no proof that this behavior is asymptotic. On the other hand the Lévy walk model predicts $\langle p(x=0, t|x=0, t=0) \rangle \sim t^{-1/\gamma}$ [6].

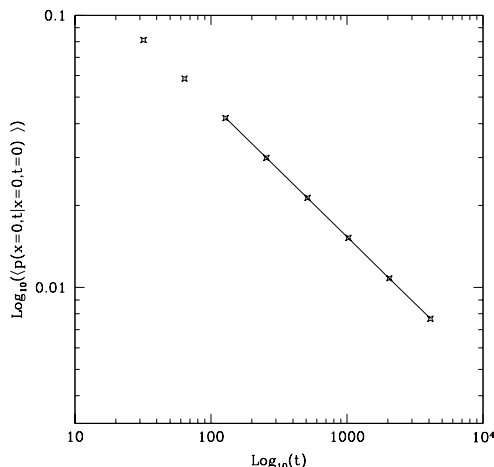


FIG. 7. $\log_{10}[\langle p(x=0, t|x=0, t=0) \rangle]$ versus $\log_{10}(t)$. The points are numerical results. The straight curve is a fit exhibiting the $t^{-1/2}$ behavior.

IV. SUMMARY AND DISCUSSION

In this work we have considered a one dimensional Lévy-Lorentz gas. We have shown that:

(a) the mean square displacement in the Lévy-Lorentz

gas is compatible with the Lévy walk framework and not with the FFPE.

(b) Ballistic contributions to the mean square displacement are important even for large times.

(c) The ballistic peaks at $x = +t$ and $x = -t$ can be analyzed analytically. They decay as power laws.

(d) The way in which the system is prepared at $t = 0$ (i.e., equilibrium versus non equilibrium initial conditions) determines the behavior of the ballistic peaks. Since these peaks contribute to the mean square displacement even at large times, we conclude that the diffusion coefficient D_δ is sensitive to the way the system is prepared.

In our work we considered an initial condition $v = 1$ or $v = -1$ with equal probabilities. It is clear that if we assign a velocity $v = +1$ to the light particle, at $t = 0$, $\langle p(x, t|x=0, t=0) \rangle$ will never become symmetric, even approximately. Instead of the three peaks in Fig. 3 one will observe only two peaks one at $x = 0$ and the other at $x = +t$.

The reason for these behaviors in the Lévy-Lorentz gas stems from the statistical importance of ballistic paths. This is different from the systems in which diffusion is normal in which these paths are of no significance at long times. Thus, similarly to Newtonian dynamics, the system exhibits a strong sensitivity to initial conditions.

Experiments measuring diffusion phenomena usually sample data only in a scaling regime (e.g., $-\sqrt{D_1 t} < x < \sqrt{D_1 t}$). Rare events where the diffusing particle is found outside this regime are many times assumed to be of no statistical importance. Here we showed that for the Lévy-Lorentz gas rare events found in the outer most part of $\langle p(x, t|x=0, t=0) \rangle$ are of statistical importance.

Note added in proof. Recently related theoretical work on enhanced diffusion was published [24]

Acknowledgment We thank A. Aharony, P. Levitz, I. Sokolov and R. Metzler for helpful discussions.

A. Appendix A

As mentioned we use a lattice model for the simulation so that ξ is an integer. We use the transformation

$$\xi = \text{INT} \left\{ \left[\tan \left(\frac{u\pi}{2} \right) \right]^{1/\gamma} \right\} + 1. \quad (17)$$

Here $\text{I} = \text{INT}\{z\}$ is the integer closest to z satisfying $I \leq z$. In Eq. (17) u is a random variable distributed uniformly according to

$$0 \leq u_{min} \leq u \leq u_{max} \leq 1, \quad (18)$$

where u_{min} and u_{max} are cutoffs. It is easy to generate the random variable u on a computer. The probability to find an interval of length ξ is,

$$\mu(\xi) = \int_{\xi-1}^{\xi} \mu_c(y) dy \quad (19)$$

with

$$\mu_c(y) = \begin{cases} 0 & y < y_{min} \\ \frac{2\gamma}{\pi\Delta} \frac{y^{\gamma-1}}{1+y^{2\gamma}} & y_{min} < y < y_{max} \\ 0 & y > y_{max}. \end{cases} \quad (20)$$

Here

$$y_{min} = \left[\tan\left(\frac{u_{min}\pi}{2}\right) \right]^{1/\gamma}, \quad y_{max} = \left[\tan\left(\frac{u_{max}\pi}{2}\right) \right]^{1/\gamma} \quad (21)$$

are the cutoffs of $\mu_c(y)$. When $u_{min} = 0$ and $u_{max} = 1$ we have $y_{min} = 0$ and $y_{max} = \infty$. In Eq. (20) $\Delta = u_{max} - u_{min}$ determines the normalization condition $\int_0^{\infty} \mu_c(y) dy = 1$.

To derive Eqs. (19)-(21) we use the transformation $y = [\tan(u\pi/2)]^{1/\gamma}$, and then $\mu_c(y) = g(u) |du/dy|$, where $g(u)$ is the uniform probability density of u .

For large ξ we find

$$\mu(\xi) \sim \begin{cases} \frac{2\gamma}{\pi\Delta} \xi^{-1-\gamma} & \xi < \xi_{max} \\ 0 & \xi > \xi_{max}, \end{cases} \quad (22)$$

with $\xi_{max} = \text{INT} \left\{ [\tan(u_{max}\pi/2)]^{1/\gamma} \right\} + 1$. When $u_{max} = 1$ the second moment of $\mu(\xi)$ diverges.

In our numerical simulations we consider $u_{min} = 1/2$, $u_{max} = 1$ and $\gamma = 3/2$. Then $\langle \xi \rangle \simeq 4.031$ and for large ξ , we find

$$\mu(\xi) \sim (6/\pi) \xi^{-5/2} \quad \xi \gg 1. \quad (23)$$

B. Appendix B

The calculation of $\hat{Q}_b(u)$ can be found in [19,22]. The probability that the interval $(0, t)$ is empty is

$$G_0(t) = 1 - \int_0^t h(\tau) d\tau \quad (24)$$

and in Laplace space $\hat{G}_0(u) = [1 - \hat{h}(u)]/u$. The Laplace transform of $G_r(t)$ for $r \geq 1$ is found using convolution

$$\hat{G}_r(u) = \hat{h}(u) \hat{\mu}^{r-1}(u) \hat{W}(u). \quad (25)$$

$W(t) = 1 - \int_0^t \mu(\xi) d\xi$ is the probability that an interval of length $(0, t)$ is empty, given that a scatterer occupies 0^- . In Laplace space $\hat{W}(u) = [1 - \hat{\mu}(u)]/u$. Using Eqs. (24), (25) and (7) we find (8).

Author e-mail: barkai@mit.edu

- 1 J. P. Bouchaud and A. Georges, *Phys. Rep.* **195** 127 (1990).
- 2 M.F. Shlesinger, G. M. Zaslavsky and U. Frisch ed. *Lévy Flights and Related Topics in Physics* (Springer-Verlag, Berlin, 1994).
- 3 J. Klafter, M. F. Shlesinger and G. Zumofen, *Physics Today* **49** (2) 33 (1996).
- 4 E. Barkai and J. Klafter, in *Chaos, Kinetics and Non-linear Dynamics in Fluids and Plasmas* G. M. Zaslavsky and S. Benkadda ed. (Springer-Verlag, Berlin 1998).
- 5 T. Geisel, J. Nierwetberg and A. Zacherl, *Phys. Rev. Lett.* **54**, 616 (1985).
- 6 G. Zumofen and J. Klafter, *Phys. Rev. E* **47**, 851 (1993).
- 7 T. H. Solomon, E. R. Weeks and H. L. Swinney, *Phys. Rev. Lett.* **71**, 23 (1995).
- 8 A. Torcini and M. Antony, *Phys. Rev. E* **57**, R6233 (1998).
- 9 Matsuoka and R. F. Martin, *J. Stat. Phys.* **88** 81 (1997).
- 10 T. Geisel, A. Zacharel and G. Radons *Z. Phys. B* **71** 117 (1988).
- 11 P. Levitz, *Europhys. Lett.* **39** 6 593(1997).
- 12 P. Levitz and D. Tchoubar, *J. Phys. I* **2** 771 (1992).
- 13 H. van Beijeren, *Rev. Mod. Phys.* **54** 195 (1982).
- 14 P. Grassberger, *Physica A* **103** 558 (1980).
- 15 H. van Beijeren and H. Spohn, *J. Stat. Phys.* **31** 231 (1983).
- 16 M. H. Ernst, J. R. Dorfman, R. Nix and D. Jacobs *Phys. Rev. Lett.* **74** 4416 (1995).
- 17 E. Barkai and V. Fleurov, *J. Stat. Phys.* **96**, 325 (1999).
- 18 E. Barkai and V. Fleurov, *Phys. Rev. E* **56** 6355 (1997).
- 19 W. Feller, *An introduction to probability Theory and Its Applications* Vol. 2 (John Wiley and Sons 1970).
- 20 I. M. Sokolov, J. Mai and A. Blumen, *Phys. Rev. Lett.* **79** 857 (1997).
- 21 M. Stefancich, P. Allegrini, L. Bonci, P. Grigolini and B. J. west *Phys. Rev. E* **57** 6625 (1998)
- 22 D. R. Cox, *Renewal Theory*, (Methuen & Co. London, 1970).
- 23 H. C. Fogedby, *Phys. Rev. Lett.* **73** 2517 (1994), *Phys. Rev. E* **58** 1690 (1998).
- 24 V. Latora, P. Rapisarda and S. Ruffo *Phys. Rev. Lett.* **83** 2104 (1999), B.A. Carreras, V.E. Lynch, D.E. Newman and G. M. Zaslavsky *Phys. Rev. E* **69** 4770 (1999), P. Castiglione, A. Mazzino, P. Muratore-Ginanneschi and A. Vulpiani *Physica D* **134** 75 (1999)